Cilostazol attenuates ischemia-reperfusion-induced blood-brain barrier dysfunction enhanced by advanced glycation endproducts via transforming growth factor - β1 signaling.

Tomonori Takeshita [a], Shinsuke Nakagawa [b,c,*], Rie Tatsumi [b], Gohei So [a], Kentaro Hayashi [a], Kunihiko Tanaka [b], Maria A. Deli [d], Izumi Nagata [a], Masami Niwa [b, c, 1]

[a] *Department of Neurosurgery, Nagasaki University Graduate School of Biomedical Sciences, 1-7-1 Sakamoto, Nagasaki 852-8501, Japan*

[b] *Department of Pharmacology, Nagasaki University Graduate School of Biomedical Sciences, 1-12-4 Sakamoto, Nagasaki 852-8523, Japan*

[c] *BBB Laboratory, PharmaCo-Cell Company, Ltd., Nagasaki, 1-43 Dejima, Nagasaki 850-0862, Japan*

[d] *Laboratory of Molecular Neurobiology, Institute of Biophysics, Biological Research Center, Hungarian Academy of Sciences, Temesvári körút 62, H-6726 Szeged, Hungary*

[1] *Professor emeritus at Nagasaki University*

* Corresponding author: S. Nakagawa; Fax: +81-95-819-7044
E-mail: shin3@nagasaki-u.ac.jp

Abbreviations used: AGEs, advanced glycation endproducts; BBB, blood-brain barrier; BSA, bovine serum albumin; CARASIL, cerebral autosomal recessive arteriopathy with subcortical infarcts and leukoencephalopathy; DMEM, Dulbecco's modified Eagle's medium; GFAP, glial fibrillary acidic protein; OGD, oxygen glucose deprivation; PDE, phosphodiesterase; PBS, phosphate-buffered saline; PDS, plasma derived from serum; PKA, protein kinase A; RBEC, rat brain capillary endothelial cells; RAGE, receptor for AGEs; TJs, tight junctions; TEER, transendothelial electrical resistance; TGF, transforming growth factor; ZO-1, zonular occludens-1

Abstract

We investigated the effects of cilostazol, a selective inhibitor of phosphodiesterase 3, on blood-brain barrier (BBB) integrity against ischemia-reperfusion injury enhanced by advanced glycation endproducts (AGEs). We used *in vitro* BBB models with primarily cultured BBB-related cells from rats (brain capillary endothelial cells, astrocytes and pericytes), and subjected cells to either normoxia or 3-h oxygen glucose deprivation (OGD)/24-h reoxygenation with or without AGEs. Treatment of AGEs did not affect the transendothelial electrical resistance (TEER) in the BBB model under normoxia, but there was a significant decrease in TEER under 3-h OGD/24-h reoxygenation conditions with AGEs. Cilostazol inhibited decreases in TEER induced by 3-h OGD/24-h reoxygenation with AGEs. Immunocytochemical and Western blot analyses showed that AGEs reduced the expression of claudin-5, the main functional protein of tight junctions (TJs). In contrast, cilostazol increased the expression of claudin-5 under 3-h OGD/24-h reoxygenation with AGEs. Furthermore, while AGEs increased the production of extracellular transforming growth factor (TGF)-β1, cilostazol inhibited the production of extracellular TGF-β1 and restored the integrity of TJs. Thus, we found that AGEs enhanced ischemia-reperfusion injury, which mainly included decreases in the expression of proteins comprising TJs through the production of TGF-β1. Cilostazol appeared to limit ischemia-reperfusion injury with AGEs by improving the TJ proteins and inhibiting TGF-β1 signaling.

Keywords: cilostazol, blood-brain barrier, claudin-5, oxygen glucose deprivation/reoxygenation, advanced glycation endproducts, transforming growth factor-β

Introduction

The prevalence of diabetes is increasing rapidly worldwide and is a major cause of morbidity and mortality (Guariquata et al., 2011), with diabetic angiopathy having a particularly serious effect on quality of life and mortality of diabetic patients (Vinik and Flemmer, 2002). Diabetic angiopathy can be classified into atherosclerotic macrovascular disease affecting the arteries that supply the heart, brain and lower extremities and diabetes-specific microvascular disease in the retina, glomerulus and vasa nervorum (Brownlee, 2001). The dysfunction of vascular endothelial cells is considered to be a key initial step in diabetic angiopathy, and to affect the progression and severity of diabetes. Four main molecular mechanisms (increased polyol pathway flux, increased advanced glycation endproducts (AGEs) formation, activation of protein kinase C isoforms, and increased hexosamine pathway flux) appear to cause diabetic microvascular and macrovascular pathologies and all result from hyperglycemia (Brownlee, 2001). Among these, we focused on AGEs, which affect vascular endothelial cells in diabetes, as AGEs are considered to be an important factor in the formation of diabetic vascular complications (Basta et al., 2004). We also evaluated the effects of AGEs on ischemic stroke by administrating AGEs under hypoxia reperfusion conditions.

While it is well known that diabetes enhances infarct volume and cerebral edema (Vannucci et al., 2001; Tureyen et al., 2011), the detailed mechanisms by which diabetes exerts damage on brain microvascular endothelial cells remain unknown. We speculated that AGEs play an important role in the deterioration of the cerebral infarct in diabetes. AGEs are formed by non-enzymatic reactions between reducing sugars and free amino groups of proteins that undergo complex and irreversible molecular rearrangement. AGEs activate RhoA in endothelial cells, leading to increased hyperpermeability through actin polymerization (Hirose et al., 2010),

and increase permeability and vascular endothelial growth factor mRNA expression in brain microvascular endothelial cells (Niiya et al., 2012). Moreover, recent studies have revealed that the receptor for AGEs (RAGE) is the main receptor for amyloid-beta peptide transport across the blood-brain barrier (BBB) from blood to brain and is a potential target for Alzheimer's disease therapy (Deane et al., 2009). Yamagishi et al. (1998) showed that AGEs decreased cyclic AMP concentrations in endothelial cells, while Ishizaki et al. (2003) reported that cyclic AMP induces expression of the claudin-5 gene in BBB endothelial cells. Accordingly, we suggested that cAMP and the protein kinase A (PKA) pathway are closely related to AGE-induced pathophysiology and that they play an important role in the treatment of AGE-related cerebral ischemia.

Cilostazol, a selective inhibitor of phosphodiesterase (PDE) 3, increases intracellular cyclic AMP concentrations. Cilostazol has been approved for use as a vasodilating and antiplatelet drug for the treatment of ischemic symptoms in chronic peripheral arterial obstruction and secondary prevention of cerebral infarction. Recently, cilostazol has been shown to be a more effective and safer alternative to aspirin for long-term prevention of the recurrence of ischemic stroke in patients with chronic ischemic stroke (Shinohara et al., 2010). In addition, increasing evidence has shown that cilostazol also exerts a protective effect by promoting BBB integrity (Torii et al., 2007, Horai et al., 2013).

AGEs appear to be an important factor for the development of diabetic retinopathy and nephropathy, but the detailed mechanisms by which AGEs induce disruption of the BBB during diabetic cerebral microvascular disease remain unclear. A recent study has suggested that AGEs activate transforming growth factor (TGF) - β to cause renal and vascular disease (Li et al., 2004). Shimizu et al. (2011, 2013) found that AGEs stimulated the release of TGF-β by pericytes. The TGF-β family is involved in many cellular processes, including cell growth, cell

differentiation, migration, apoptosis, cellular homeostasis and other cellular functions, in both the developing embryo and the adult organism (Beck and Schachtrup, 2011). However, excess TGF-β signaling is induced in the neurovascular unit upon central nervous system injury and disease with BBB rupture. Hara et al. (2009) reported that this increased TGF-β signaling causes cerebral arteriopathy in cerebral autosomal recessive arteriopathy with subcortical infarcts and leukoencephalopathy (CARASIL). CARASIL is characterized by ischemic, non-hypertensive, cerebral small vessel disease with associated alopecia and spondylosis, and magnetic resonance imaging demonstrated homogeneously confluent white matter changes and multiple lacunar infarctions in the basal ganglia and thalamus. Therefore, we suggested that TGF-β signaling is closely associated with BBB impairment induced by AGEs.

In the present study, we clarified the effects of AGEs on the BBB and the underlying mechanisms by analyzing tight junction (TJ) proteins and factors affecting endothelial cells. Furthermore, we examined the effects of cilostazol on the BBB after exposure to AGEs under hypoxia reperfusion conditions.

Results

Transendothelial Electrical Resistance (TEER) in BBB Model Treated with AGEs

Transendothelial electrical resistance (TEER) in the BBB model was more than 150 $\Omega \times cm^2$. To analyze the potential harmful effects of AGEs on BBB integrity, we measured TEER under normoxia with or without AGEs. Treatment of AGEs (200 μg/mL, incubation at 37°C) under normoxia had no effect on TEER in the co-culture model. In contrast, treatment of AGEs under normoxia decreased the TEER when compared with BSA-control (200 μg/mL) at 24 h (TEER

(% of normoxia BSA-control) BSA: 100.0 ± 1.9 vs. AGEs: 98.3 ± 1.2) (Fig. 2A). In contrast, AGEs significantly decreased TEER when compared with BSA-control after 3-h OGD/24-h reoxygenation experiments (Fig. 2A). To determine the possible molecular mechanisms of hypoxia reperfusion injury on rat brain endothelial cells, we compared the expression of RAGE under normoxia with 3-h OGD/24-h reoxygenation conditions. Our results showed that expression of RAGE was significantly elevated after 3-h OGD/24-h reoxygenation, as compared with that under normoxia (Fig. 2B). As the effects of AGEs were observed at 200 μg/mL under 3-h OGD/24-h reoxygenation conditions, these concentrations and conditions were used in subsequent experiments.

Effects of Cilostazol on Barrier Function of BBB Model

Next, we investigated the effects of cilostazol against AGE-induced BBB impairment. The treatment of cilostazol (10 μM) under normoxia had no effect on TEER when compared with BSA-control at 24 h (TEER (% of BSA-control); cilostazol: 93.8 ± 3.2 vs. BSA: 100.0 ± 5.0). In contrast, Liu et al. (2012) and Horai et al. (2013) reported that cilostazol strengthened TEER in brain capillary endothelial cells. This discrepancy may have been due to differences in the concentration of cilostazol, incubation time or cell culture conditions. Treatment with cilostazol significantly increased TEER after 3-h OGD/24-h reoxygenation experiments with AGE (TEER (% of normoxia BSA-control); AGEs + cilostazol: 100.8 ± 10.6 vs. AGEs: 65.6 ± 8.4; $p < 0.01$) (Fig. 3).

Effects of AGEs on Claudin-5 and ZO-1 Expression under 3-h OGD/24-h reoxygenation

Our immunocytochemical study revealed continuous and linear staining for claudin-5 and ZO-1, a key protein composing TJs, marginally localized in the cell border between RBEC of BSA-control under normoxia (Fig. 4A, E). Microscopic observation revealed no significant differences in fluorescence intensity for claudin-5, but morphological distribution differed in RBEC treated with BSA under 3-h OGD/24-h reoxygenation (Fig. 4B). Discontinuous localization of claudin-5 could be observed in RBEC treated with AGEs under 3-h OGD/24-h reoxygenation (Fig. 4C). Treatment with cilostazol increased the expression of claudin-5, leading to continuous, smooth patterns (Fig. 3D). In contrast, no significant changes were observed in the expression of ZO-1 after exposure to AGEs under 3-h OGD/24-h reoxygenation (Fig. 4E-H). Changes in the expression of claudin-5 and ZO-1 levels in *in vitro* BBB models treated with AGEs under 3-h OGD/24-h reoxygenation were investigated by Western blot analyses. While treatment with AGEs under 3-h OGD/24-h reoxygenation apparently decreased the expression of claudin-5 when compared with BSA under normoxia, treatment with cilostazol restored the expression of the claudin-5 (Fig. 4I). However, there were no differences in expression of ZO-1 in *in vitro* BBB models (Fig. 4J).

Involvement of TGF-β1 on AGE-induced BBB Dysfunction under OGD and Reoxygenation

In order to examine the functional association between AGEs and TGF-β1 levels, we measured the extracellular TGF-β1 concentration in BBB models treated with AGEs. As shown in Fig. 5A, treatment with AGEs were found to markedly increase TGF-β1 concentrations when compared with BSA under 3-h OGD/24-h reoxygenation (454.6 ± 7.2 pg/mL vs. 397.0 ± 4.9 pg/mL; $P<0.01$). On the other hand, cilostazol decreased TGF-β1 concentrations when compared with AGEs under 3-h OGD/24-h reoxygenation. These results suggest that production

of TGF-β1 was increased by AGEs under 3-h OGD/24-h reoxygenation, and that cilostazol is able to regulate TGF-β1 production. Next, we used an inhibitor of TGF-β type I receptor to block the AGE-TGF-β interaction. A83-01 is a selective inhibitor of the TGF-β type I receptor ALK5, the Activin/Nodal receptor ALK4, and the nodal receptor ALK7. A83-01 elevated TEER, which was decreased by AGEs under 3-h OGD/24-h reoxygenation (TEER (% of normoxia BSA-control); AGEs + A83-01: 74.9 ± 7.7 vs. AGEs: 50.1 ± 2.9; $P<0.01$), while no significant differences were observed between BSA and BSA treated with A83-01 (Fig. 5B).

Effects of TGF-β1 on BBB Model

In order to examine the effects of TGF-β1 on the barrier function of the BBB, we administered TGF-β1 to the BBB model. Treatment of recombinant TGF-β1 (1 ng/mL, incubation at 37°C) significantly decreased TEER in a time-dependent manner when compared with controls, and cilostazol was able to inhibit the decrease in TEER induced by TGF-β1 (Fig. 6).

Discussion

In the present study, we demonstrated that AGEs enhance ischemia-reperfusion injury, which mainly includes decreases in the expression of proteins comprising TJs through TGF-β1 signaling. Cilostazol reduced ischemia-reperfusion injury with AGEs by improving TJ proteins and inhibiting TGF-β1 signaling.

The BBB forms a neurovascular unit that protects the brain from circulating neurotoxic agents and inflammatory factors while maintaining nutrients and ions in the brain at levels

suitable for brain function (Yan et al., 2012). The BBB is composed of microvascular endothelial cells surrounded by pericytes and the astrocyte foot process. The integrity of endothelial cell-cell junctions is regulated by a series of adhesion molecules that make up TJs. Tsukita et al. (2001) revealed that claudin is an important adhesion molecule among the TJ proteins. Claudin-5 is particularly elevated in TJs in vascular endothelial cells and is associated with the maintenance of normal BBB function (Cardoso et al., 2010). Zonula occludens protein-1 (ZO-1), ZO-2, and ZO-3 are exclusively concentrated at the cytoplasmic surface of TJs in the immediate vicinity of plasma membranes, and are bound to claudin (Itoh et al., 1999). Pericytes are important cellular constituents of the capillaries and post-capillary venules, having a close physical association with endothelial cells (Dore-Duffy, 2008). Armulik et al. (2010) demonstrated that pericytes in the BBB function in at least two ways: regulating BBB-specific gene expression patterns in endothelial cells, and inducing polarization of the astrocyte foot process surrounding central nervous system blood vessels. Astrocytes are glial cells whose foot process forms a lacework of fine lamellae closely apposed to the outer surface of endothelial cells. Perivascular astrocytes could be in partnership with endothelial cells, leading to a complex cell-cell exchange of chemical signals, inducing BBB features and modulating cellular physiology (Abbott, 2002). The cross-talk among cells comprising the neurovascular unit is crucial for the formation and maintenance of the BBB. Accordingly, we used the triple co-culture BBB model (Fig. 1) because this *in vitro* BBB model corresponds to the anatomical and physiological situation in the cerebral microvessels *in vivo*, as compared with the monolayer model of brain microvascular endothelial cells. Some reports have indicated that AGEs increase the permeability of the brain endothelial cell monolayer under non-ischemic conditions (Niiya et al., 2012, Shimizu et al., 2013). In agreement with these observations, the TEER value of our cultured RBEC monolayer decreased by treatment of AGEs (200 μg/mL)

under non-ischemic conditions (data not shown). However, we could not confirm that AGEs affected the permeability of brain capillary endothelial cells in our triple co-culture model under normoxia. These observations suggest that cross-talk among cells comprising the BBB influences AGE/RAGE interaction via an unknown mechanism.

Diabetes is considered to be both a metabolic disease and a vascular disease because of its effects on macro- and microcirculation in numerous vascular beds, including cerebral vessels. Generally, diabetes or chronic hyperglycemia contributes to proliferation of vascular smooth muscle cells, degeneration of endothelial cells and pericytes, thickening of the capillary basement membrane, and an increase in aggregation and adhesion of platelets to the endothelium (Ergul et al., 2009). Accumulating evidence has indicated that AGEs increase at an accelerating rate in diabetes and in parallel with the severity of diabetic complications (Hirose et al., 2010). AGEs are able to mediate diabetic complications by stimulating a number of mediators, including oxygen free radicals, cytokines, chemokines, adhesion molecules, TGF-β1 and connective tissue growth factor (Chung et al., 2010). Vannucci et al. (2001) and Tureyen et al. (2011) have reported that a model of type-2 diabetes mouse that subjected to focal ischemia showed significantly higher mortality, bigger infarcts, increased cerebral edema and worsened neurological status as compared to nondiabetic animals. Diabetes exacerbates cerebral infarcts because hyperglycemia enhances superoxide anion radical generation in the blood, thereby increasing oxidative stress, early inflammation and endothelial injury after forebrain ischemia/reperfusion in rats (Tsuruta et al., 2010), and increasing the permeability of endothelial cells comprising the BBB (Allen and Bayraktutan, 2009, Hawkins et al., 2007). Starr et al. (2003) reported hyperpermeability of the BBB in type II diabetes on gadolinium magnetic resonance imaging. Our findings showed that AGEs further decrease TEER under OGD and reoxygenation conditions, as compared with normoxia, and these results support the notion that

ischemia reperfusion injury in diabetes enhances the impairment of BBB integrity *in vivo*. RAGE is present in minimal quantities in normal endothelial cells, but is upregulated in a positive-feedback manner when AGE ligands accumulate. These activities may induce inflammatory responses, leading to aggravation of diabetic vascular complications (Shimizu et al., 2011). Our results also indicated the up-regulation of RAGE expression under OGD and reoxygenation. Furthermore, several studies have suggested that the expression of RAGE in endothelial cells is elevated under OGD and reoxygenation (Yan et al., 2008, Zhai et al., 2008). Therefore, increased RAGE under ischemia-reperfusion is involved in the dysfunction of the BBB caused by AGEs. The enhanced interaction between AGEs and RAGE may accelerate inflammatory reactions, and worsen cerebral infarcts.

In order to elucidate the changes in TJ proteins after exposure to AGEs under OGD and reoxygenation, we examined the expression of claudin-5 and ZO-1 in RBEC in the BBB model. Claudin-5 is known to be the main structure responsible for the barrier properties of the BBB, and is thought to be closely related to the tightness of BBB integrity with a high TEER (Nitta et al., 2003; Furuse and Tsukita 2006; Koto et al., 2007; Tsukita et al., 2008). The present immunocytochemical and Western blot analyses indicated that AGEs reduced the expression of claudin-5 in RBEC. In contrast to the expression of claudin-5, ZO-1 in the immunocytochemical and Western blot analysis did not differ after exposure to AGEs under OGD and reoxygenation. Taken together with the previous report that the TEER was closely related to the amount of claudin-5 expressed as a TJ protein (Koto et al., 2007), AGE-induced BBB impairment under OGD and reoxygenation is mainly associated with decreased expression of claudin-5.

Among the mediators stimulated by AGEs, TGF-β1 was related to disrupting the blood-nerve barrier and BBB in diabetic neuropathy (Shimizu et al., 2011, 2013) and the development of glomerulosclerosis in diabetic nephropathy (Chung et al., 2010). In this study, we investigated

whether TGF-β1 signaling contributes to the impairment of the BBB after exposure to AGEs. We detected a significant increase in TGF-β1 release from RBEC subjected to OGD and reoxygenation. Furthermore, AGEs led to enhanced extracellular TGF-β1 concentrations under OGD and reoxygenation. In addition, the treatment of TGF-β1 significantly decreased TEER in a time-dependent manner when compared with controls in RBEC. TGF-β1 secretion from RBEC, which is elevated by AGEs under OGD and reoxygenation, works on neighboring endothelial cells as an autocrine factor. These data are in agreement with a recent study showing that TGF-β increased the permeability of brain capillary endothelial cells (Shen et al., 2011). We observed that AGEs worked on RBEC to significantly decrease TEER, but this effect was inhibited by A83-01, a selective inhibitor of the TGF-β type I receptor ALK5, the Activin/Nodal receptor ALK4, and the nodal receptor ALK7. To the best of our knowledge, this is the first report regarding the relationship between AGEs and TGF-β1 signaling in the barrier integrity of the BBB under ischemic conditions. Our results suggested that the increase in TGF-β1 signaling was closely associated with impairment of the BBB after exposure to AGEs under OGD and reoxygenation. The inhibition of pathological response mediated by TGF-β1 signaling may represent a therapeutic target for diabetic cerebral vessel disease. However Dohgu et al. (2005) and Ronaldson et al. (2009) indicated that TGF-β has beneficial effects on BBB function under physiological and pathological pain conditions, respectively. Therefore, TGF-β appears to have different effects on BBB function, depending on physiological and pathological conditions.

We clarified that cilostazol protected BBB integrity against AGE-induced impairment under OGD and reoxygenation. It is known that cAMP plays an important role in stabilizing the barrier properties of endothelial cells (Ishizaki et al., 2003; Deli et al., 2005; Noda et al., 2010), and Yamahishi et al., (1998) reported that AGEs decrease cAMP concentrations in endothelial cells. Cilostazol is a selective inhibitor of PDE3, and accordingly, it increases intracellular

cAMP contents and activates PKA (Hashimoto 2006). Horai et al. (2013) indicated that cilostazol elevated intracellular cAMP levels in RBEC and improved BBB integrity via the cAMP/PKA pathway. These findings suggest that cilostazol has potential as a protective drug against AGE-induced BBB dysfunction. In the present study, cilostazol enhanced the expression of claudin-5 and TEER values in RBEC treated with AGEs under OGD and reoxygenation. Thus, cilostazol appears to protect the barrier function of the BBB, presumably through the cAMP/PKA pathway when AGEs reduce cAMP concentration in RBEC under OGD and reoxygenation.

Recent evidence has shown that diabetic rats treated with cilostazol effectively prevented the up-regulation of TGF-β1 expression in the kidney compared with untreated rats (Wang et al., 2009). We therefore hypothesized that cilostazol contributes to the suppression of TGF-β1 activation in the BBB. In the present study, our findings indicated that cilostazol decreases extracellular TGF-β1 concentrations after exposure to AGEs under OGD and reoxygenation. These results suggest that cilostazol prevents AGE-mediated BBB dysfunction by reducing TGF-β1 production or activation. Furthermore, cilostazol improved BBB dysfunction induced by the treatment of recombinant TGF-β1 in the *in vitro* BBB model. As it has been reported that increased cAMP levels antagonize the inductive effects of TGF-β on fibroblasts (Togo et al., 2009; Schiller et al., 2010), increases in intracellular cAMP levels by cilostazol may be involved in the protective effects of cilostazol.

In summary, AGEs reduced the barrier integrity of the *in vitro* BBB model under OGD and reoxygenation conditions, as compared with normoxia, and this effect may be due to the up-regulation of RAGE expression. AGEs enhanced ischemia-reperfusion injury, which decreased with the expression of claudin-5 containing TJs, and increased with TGF-β1 signaling. Cilostazol appears to improve ischemia-reperfusion injury enhanced by AGEs through the

inhibition of TJ protein disruptions by reducing the effects of TGF-β1 on brain capillary endothelial cells. The present study suggests that cilostazol is able to act as a BBB-protective drug for diabetic cerebral vessel disease.

Experimental methods

Reagents and Animals

Cilostazol (6-[4-(1-cyclohexyl-1*H*-tetrazol-5yl)butoxy]-3,4-dihydroquinolin-2-(1*H*)-one, MW 369.46) was kindly provided by Otsuka Pharmaceutical Co., Ltd. (Tokushima, Japan). Cilostazol was dissolved to a concentration of 20 mM in Dimethyl sulfoxide, stored at -20°C and diluted with medium when the experiment was performed. All reagents and drugs were purchased from Sigma-Aldrich (St. Louis, MO, USA), unless otherwise indicated. Wistar rats were obtained from Japan SLC Inc. (Hamamatsu, Japan). All animals were treated in strict accordance with NIH Guidelines for the Care and Use of Laboratory Animals (NIH Publication Nos. 80-23), and all protocols were approved by the Nagasaki University Animal Care Committee.

Cell cultures

Primary cultures of rat brain capillary endothelial cells (RBEC) were prepared from 3-week-old rats, as described previously (Deli et al., 1997; Nakagawa et al., 2007, 2009). Meninges were carefully removed from the forebrain and gray matter was minced into small pieces of 1 mm^3 in ice-cold Dulbecco's modified Eagle's medium (DMEM), followed by

dissociation with 25 up-and-down strokes using a 5-mL pipette in DMEM containing collagenage type 2 (1 mg/mL; Worthington Biochemical Corp., Lakewood, NJ, USA), 300 μL of DNase (15 μg/mL) and gentamycin (50 μg/mL), and digestion in a shaker for 1.5 h at 37°C. Cell pellets were separated by centrifugation in 20% bovine serum albumin (BSA)-DMEM (1,000 × g, 20 min). The microvessels obtained in the pellet were further digested with collagenage-dispase (1 mg/mL; Roche Applied Sciences, Rotkreuz, Switzerland) and DNase (6.7 μg/mL in DMEM for 45 min at 37°C). RBEC clusters were separated on a 33% continuous Percoll (Pharmacia, Uppsala, Sweden) gradient, and were then collected and washed twice in DMEM before plating on 100-mm plastic dishes coated with collagen type IV (0.1 mg/mL) and fibronectin (0.1 mg/mL) (Day 0). RBEC cultures were maintained in DMEM/F12 supplemented with 10% fetal bovine plasma derived from serum (PDS) (Animal Technologies, Inc., Tyler, TX), basic fibroblast growth factor (bFGF, 1.5 ng/mL; Roche Applied Sciences), heparin (100 μg/mL), insulin (5 μg/mL), transferrin (5 μg/mL), sodium selenite (5 ng/mL) (insulin-transferrin-sodium selenite media supplement), gentamycin (50 μg/mL) and puromycin (4 μg/mL) (RBEC I medium) at 37°C under a humidified atmosphere of 5.0% CO_2/95% air for 2 days. Based on the findings of Perrière et al. (2005), in the first two days, cells were incubated in medium containing puromycin (4 μg/mL) in order to avoid contamination by pericytes. After 2 days, cells received new medium containing all the components of RBEC medium except for puromycin (RBEC II medium) (Day 2, Fig. 1). When cultures reached 80% confluence (Day 4), purified endothelial cells were passaged by brief treatment with trypsin (0.05% w/v)-EDTA (0.02% w/v) solution, and were used to construct the *in vitro* BBB model.

Rat cerebral astrocytes were obtained from neonatal Wistar rats. Meninges were removed and cortical pieces mechanically dissociated in astrocyte culture medium (DMEM supplemented with 10% fetal bovine serum). Dissociated cells were seeded into cell culture flasks. To obtain

type 1 astrocytes, flasks with confluent cultures were shaken at 37°C overnight. Astrocyte purity was confirmed by immunostaining for glial fibrillary acidic protein (GFAP), and cells were used at passage 2.

Pure cultures of rat cerebral pericytes were obtained by prolonged, 2-week culture of isolated brain microvessel fragments, which contain pericytes and endothelial cells. The same preparations yield primary RBEC after puromycin treatment. Pericyte survival and proliferation was favored by selective culture conditions using uncoated dishes, and DMEM supplemented with 10% fetal bovine serum and antibiotics. Culture medium was changed every 3 days. Pericytes were characterized by their large size and branched morphology, positive immunostaining for α-smooth muscle actin, NG2 chondrotitin sulfate proteoglycan, and absence of *von Willebrand* factor and GFAP staining. Pericytes and astrocytes were frozen in cryo-medium CELLBANKER® (Zenoaq, Koriyama, Japan), and were stored at -80°C until use.

Construction of in vitro BBB model

The day when endothelial cells were plated and models were established was defined as day four *in vitro* (day 4, Fig. 1). To construct an *in vitro* model of the BBB, pericytes (2.0×10^4 cells/cm^2) were cultured on the outside of the collagen-coated polycarbonate membrane (3.0-μm pore size; Corning Life Science, Tewksbury, MA, USA) of the Transwell inserts and astrocytes (1.0×10^5 cell/cm^2) were seeded on the bottom side of the Transwell. Cells were let to adhere firmly overnight, and endothelial cells (2.0×10^5 cells/cm^2) were seeded on the inside of the inserts placed in the well of the 12-well culture plates. From day 5, BBB models were maintained in RBEC medium II supplemented with 500 nM hydrocortisone (Hoheisel et al., 1998). Under these conditions, *in vitro* BBB models were established within 3 days after setting

of cells.

Normoxia conditions

Cells were cultured in RBEC medium II with bovine serum albumin (BSA) and AGE-BSA (AGEs) (BioVision, Mountain View, Milpitas, CA, USA). We used a dose of 200 μg/mL AGEs and 10 μM cilostazol, based on previous reports (Kikuchi et al., 2005, Liu et al., 2012, Horai et al., 2013). Cilostazol and AGEs were added into the luminal side of the BBB model. At 3 h after cilostazol and AGE treatment, medium with cilostazol and AGEs was exchanged, followed by incubation for a further 24 h, as normoxia conditions were consistent with *in vitro* oxygen glucose deprivation (OGD) and reoxygenation conditions.

In vitro OGD and Reoxygenation Studies on *in vitro* BBB model

We examined the effects of AGEs and cilostazol on *in vitro* OGD and reoxygenation-induced BBB damage. Based on our preliminary experiments, exposure times of 3 h for OGD and 24 h for reoxygenation (3-h OGD/24-h reoxygenation) were selected. For 3-h OGD/24-h reoxygenation experiments, serum-free and glucose-free DMEM (Gibco, Carlsbag, CA, USA) were added to the BBB model. Oxygen deprivation was generated using ANAEROPACK® (Mitsubishi Gas Chemical Co., Inc., Tokyo, Japan). Reoxygenation was initiated by adding RBEC II medium after 3-h OGD. Cilostazol (10 μM) and AGEs (200 μg/mL) were added to the luminal (upper) compartment of the BBB model before and after 3-h OGD. After 24-h reoxygenation, transendothelial electrical resistance (TEER) was measured, as described below (Fig. 1).

Measurement of TEER

Transendothelial electrical resistance, which reflects the flux of sodium ions through the cell layer, was measured using an EVOM resistance meter (World Precision Instruments, Sarasota, FL, USA). The extracellular matrix-treated Transwell inserts were placed in a 12-well plate containing culture medium and were then used to measure the background resistance. The resistance measurements of blank filters (background resistance) were subtracted from those filters with cells. Values are given as $\Omega \times cm^2$, and data indicate the rate of change in TEER before and after treatment in comparison with normoxia BSA.

Immunocytochemical Detection of TJ Proteins

In order to observe changes in brain endothelial TJs, BBB cells were stained with primary antibody for zonular occludens-1 (ZO-1) and claudin-5, key proteins responsible for barrier functions through the BBB (Hiu et al., 2008, Morofuji et al., 2010). All primary antibodies were used at a dilution of 1 : 200. As secondary antibodies, Alexa Flour 488 conjugated donkey anti-mouse immunoglobulins (Invitrogen Corporation, Carlsbag, CA, USA) were used at a dilution of 1 : 1000. After 3-h hypoxia and 24-h reoxygenation with or without AGE treatment, cultures were washed in phosphate-buffered saline (PBS) and fixed in 3% paraformaldehyde in PBS for 10 min and permeabilized with 0.1% Trixon-X 100 for 10 min. Cells were blocked with 3% BSA and were incubated with primary antibodies anti-ZO-1 and anti-claudin-5 (Zymed Laboratories Inc., South San Francisco, CA, USA) overnight at 4°C. Cells were rinsed with PBS, and were incubated for 1 h at room temperature with secondary antibodies (Alexa Flour

488-conjugated donkey anti-mouse immunogloblins). Between incubations, cells were washed three times with PBS. Preparations were mounted in Gel Mount (Biomeda, Foster City, CA, USA) and staining was examined using a Zeiss LSM 5 Pascal Confocal laser scanning microscope (Carl Zeiss AG, Okerkochen, Germany).

Western Blot Analysis

Cells were harvested by scraping in CelLytic™ M cell lysis reagent supplemented with proteinase inhibitor cocktail (Sigma). Lysates were centrifuged at 15,000 × g for 5 min at 4°C, supernatants were collected, and protein concentrations were determined with BCA protein assay reagent (Pierce, Rockford, IL, USA). Samples were mixed with ×6 Laemmli sample buffer, and were heated at 95°C for 5 min. An equal amount of protein for each sample was separated by 4 – 15% TGX (Tris-Glycine eXtended) gel (Bio-Rad, Hercules, CA, USA) and were then transferred onto Hybond™-P (Amersham, Buckinghamshire, UK). Non-specific binding sites were blocked with Perfect-Block (MoBiTec GmbH, Goettingen, Germany) (3% w/v) in Tris-buffered saline (25-mM Tris, 150-mM NaCl, 2-mM KCl, pH 7.4) containing 0.1% Tween-20 (TBS-T). Goat anti-RAGE polyclonal antibody (Santa Cruz Biotechnology, Inc., Paso Robles, CA, USA), anti-claudin-5 and anti-ZO-1 mouse monoclonal antibody were used at dilutions of 1 : 5,000 and anti-β actin mouse monoclonal antibody (additional loading control) was used at dilutions of 1 : 10,000, in blocking solution for 1 h at room temperature. Peroxidase-conjugated anti-goat immunoglobulin (R&D Systems, Minneapolis, MN, USA) and peroxidase-conjugated anti-mouse immunoglobulin (GE Healthcare) were used as secondary antibodies. Between incubations, blots were washed three times with TBS-T. To reveal immunoreactive bands, blots were incubated in SuperSignal West Femto Maximum Sensitivity

Substrate SECL in accordance with the manufacturer's instructions (Pierce Biotechnology, Rockford, IL, USA) and were detected using a FluorChem SP Imaging System (Alpha Innotech Corp., San Leandro, CA, USA).

Measurement of Transforming Growth Factor - beta 1 (TGF-β1)

The concentration of TGF-β1 released into cell cultured supernatants from the luminal side of the Transwell was measured by TGF-β1 immunoassay (R&D systems). A standard curve for TGF-β1 (0 to 1,000 pg/mL) was generated using recombinant TGF-β1 and the assay was performed in accordance with the supplier's recommendations. Absorbance was measured at 450 nm (Wallac 1420 ARVO Multilabel Counter, Perkin Elmer Waltham, MA, USA).

Analysis of effects of TGF-β1 on TEER and TGF-β inhibitory study

Cells were stimulated with or without 1 ng/mL recombinant human TGF-β1 (WAKO Pure Chemical Ltd., Osaka, Japan). TEER was measured at 3, 6, 9, 12, or 24 h after exposure to recombinant human TGF-β1. The *in vitro* BBB model was cultured with AGEs containing 1 ng/mL A83-01 (WAKO Pure Chemical Ltd.) under OGD/reoxygenation.

Statistical Analysis

All data are expressed as means ± standard error of the mean (SEM). Values were compared using analysis of variance followed by the Turkey-Kramer method. A p value of less than 0.05 was considered to be statistically significant.

Acknowledgments

Cilostazol was a generous gift from Otsuka Co., Ltd. (Tokushima, Japan). This work was supported in part by a Grant-in-Aid for Young Scientists (B) (24790258) from the Japan Society for the Promotion of Science (JSPS). We would like to thank Yasuko Yamashita, Keisuke Toyoda, Yoichi Morofuji, Dinh Ha Duy Thuy, Mayumi Sagara, Daisuke Watanabe and Ken Izawa for their critical reviews of the manuscript and helpful professional guidance.

References

Abbott, N. J., 2002. Astrocyte-endothelial interactions and blood-brain barrier permeability. J. Anat. 200, 629-638.

Allen, C.L., Bayraktutan, U., 2009. Antioxidants attenuate hyperglycemia-mediated brain endothelial cell dysfunction and blood-brain barrier hyperpermeability. Diabetes Obes. Metab. 11, 480-490

Armulik, A., Genove, G., Mae, M., Nisancioglu, M.H., Wallgard, E., Niaudet, C., He, L., Norlin, J., Lindblom, P., Strittmatter, K., Johansson, B.R., 2010. Pericyte regulate the blood-brain barrier. Nature 468, 562-566

Basta, G., Schmidt, A.M., De Caterina, R., 2004. Advanced glycation end products and vascular inflammation: Implications for accelerated atherosclerosis in diabetes. Cardiovasc. Res. 63, 582-592

Beck, K., Schachtrup, C., 2011. Vascular damage in the central nervous system: a multifaceted role for vascular-derived TGF-β. Cell Tissue Res. 347, 187-201

Brownlee, M., 2001. Biochemistry and molecular cell biology of diabetic complications. Nature 414, 813-820

Cardoso, F.L., Brites, D., Brito, M.A., 2010. Looking at the blood – brain barrier: molecular anatomy and possible investigation approaches. Brain Rse Rev. 64, 328-363

Chung, A.C., Zhang, H., Kong, Y.Z., Tan, J.J., Huang, X.R., Kopp, J.B., Lan, H., Y. 2010. Advanced glycation end-products induce tubular CTGF via TGF-beta-independent Smad3 signaling. J. Am. Soc. Nephrol. 21, 249-260

Deane, R., Bell, R.D., Sagare, A., Zlokovic, B.V., 2009. Clearance of amyloid-beta peptide across the blood-brain barrier: implication for therapies in Alzheimer's disease. CNS Neurol. Disord. Drug Targets 8, 16-30

Deli, M.A., Szabo, C., Dung, N., Joo, F., 1997. Immunohistochemical and electron microscopy detections on primary cultures of rat cerebral endothelial cells, in Drug transport across the blood-brain barrier: In vivo and in vitro techniques, (Boer A. G., SutantoW., eds), pp. 23-28. Harwood Academic Publishers, Amsterdam.

Deli, M.A., Abraham, C.S., Kataoka, Y., Niwa, M., 2005. Permeability studies on in vitro blood-brain barrier models: physiology, pathology, and pharmacology. Cell. Mol. Neurobiol. 25, 59-127

Dohgu, S., Takata, F., Yamauchi, A., Nakagawa, S., Egawa, T., Naito, M., Tsuruo, T., Sawada, Y., Niwa, M., Kataoka, Y., 2005. Brain pericytes contribute to the induction and up-regulation of blood-brain barrier functions through transforming growth factor-beta production. Brain Res. 1038, 208-215

Dore-Duffy, P., 2008. Pericytes: pluripotent cells of the blood brain barrier. Curr Pharm Des 14, 1581-1593

Erqul, A., Li, W., Elqebaly, M.M., Bruno, A., Faqan, S.C., 2009. Hyperglycemia, diabetes and stroke: focus on the cerebrovasculature. Vascul. Pharmacol. 51, 44-49

Furuse, M., Tsukita, S., 2006. Claudins in occluding junctions of humans and flies. Trends Cell Biol. 16, 181-188

Guariquata, L., Whiting, D., Weil, C., Unwin, N., 2011. The international diabetes federation diabetes atlas methodology for estimating global and national prevalence of diabetes in adults. Diabetes Res. Clin. Pract. 94, 322-332

Hara, K., Shiga, A., Fukutake, T., Nozaki, H., Miyashita, A., Yokoseki, A., Kawata, H., Koyama, A., Arima, K., Takahashi, T., Ikeda, M., Shiota, H., Tamura, M., Shimoe, Y., Hirayama, M., Arisato,

T., Yanagawa, S., Tanaka, A., Nakano, I., Ikeda, S., Yoshida, Y., Yamamoto, T., Ikeuchi, T., Kuwano, R., Nishizawa, M., Tsuji, S., Onodera, O., 2009. Association of HTRA1 mutations and familial ischemic cerebral small-vessel disease. N. Engl. J. Med. 360, 1729-1739

Hashimoto, A., Miyakoda, G., Hirose, Y., Mori, T., 2006. Activation of endothelial nitric oxide synthase by cilostazol via a cAMP/protein kinase A- and phosphatidyllinositol 3-kinase/Akt-dependent mechanism. Atherosclerosis 189, 350-357

Hawkins B.T., Lundeen T.F., Norwood K.M., Brooks H.L., Egleton R.D., 2007. Increased blood-brain barrier permeability and altered tight junctions in experimental diabetes in the rat: contribution of hyperglycemia and matrix metalloproteinases. Diabetologia. 50, 202-211

Hiu, T., Nakagawa, S., Hayashi, K., Kitagawa, N., Tsutsumi, K., Kawakubo, J., Honda, M., Suyama, K., Nagata, I., Niwa, M., 2008. Tissue plasminogen activator enhances the hypoxia/reoxygenation-induced impairment of the blood-brain barrier in a primary culture of rat brain endothelial cells. Cell. Mol. Neurobiol. 28, 1139-1146

Hirose, A., Tanikawa, T., Mori, H., Okada, Y., Tanaka, Y., 2010. Advanced glycation end products increase endothelial permeability through the RAGE/Rho signal pathway. FEBS Lett. 584, 61-66

Hoheisel, D., Nitz, T., Franke, H., Wegener, J., Hakvoort, A., Tilling, T., Galla, H.J., 1998. Hydrocortisone reinforces the blood-brain barrier properties in a serum free cell culture system. Biochem. Biophys. Res. Commun. 244, 312-316

Horai, S., Nakagawa, S., Tanaka, K., Morofuji, Y., Couraud, P.O., Deli, M.A., Ozawa, H., Niwa, M., 2013. Cilostazol strengthens barrier integrity in brain endothelial cells. Cell. Mol. Neurobiol. 33, 291-307

Ishizaki, T., Chiba, H., Kojima, T., Fujibe, M., Soma, T., Miyajima, H., Nagasawa, K., Wada, I., Sawada, N., 2003. Cyclic AMP induces phospholylation of claudin-5 immunoprecipitates and expression of claudin-5 gene in blood-brain-barrier endothelial cells via protein kinase A-dependent and –independent pathways. Exp. Cell Res. 290, 275-288

Itoh, M., Furuse, M., Morita, K., Kubota, K., Saitou, M., Tsukita, S., 1999. Direct binding of three tight junction - associated MAGUKs, ZO-1, ZO-2, and ZO-3, with the COOH termini of claudins. J. Cell Biol. 13, 147-163

Koto, T., Takubo, K., Ishida, S., Shinoda, H., Inoue, M., Tsubota, K., Okada, Y., Ikeda, E., 2007. Hypoxia disrupts the barrier function of neural blood vessels through changes in the expression of claudin-5 in endothelial cells. Am. J. Pathol. 170, 1389-1397

Kikuchi, Y., Imakiire, T., Hyodo, T., Kushiyama, T., Higashi, K., Hyodo, N., Suzuki, S., Miura, S., 2005. Advanced glycation end-product induces fractalkine gene upregulation in normal rat glomeruli. Nephrol. Dial. Transplant. 20, 2690-2696

Li, J.H., Huang, X.R., Zhu, H.J., Oldfield, M., Cooper, M., Truong, L.D., Johnson, R.J., Lan, H.Y., 2004. Advanced glycation end products activate Smad signaling via TGF-beta-dependent and independent mechanisms: implications for diabetic renal and vascular disease. FASEB J. 18, 176-178

Li, Q., Liu, H., Du, J., Chen, B., Li, Q., Guo, X., Huang, X., Huang, Q., 2011. Advanced glycation end products induce moesin posphorylation in murine brain endothelium. Brain Res. 1373, 1-10

Liu, S., Yu, C., Yang, F., Paganini-Hill, A., Fisher, M.J., 2012. Phosphodiesterase inhibitor modulation of brain microvascular endothelial cell barrier properties. J. Neurol. Sci. 320, 45-51.

Morofuji, Y., Nakagawa, S., So, G., Hiu, T., Horai, S., Hayashi, K., Tanaka, K., Suyama, K., Deli, M.A., Nagata, I., Niwa, M., 2010. Pitavastatin strengthens the barrier integrity in primary cultures of rat brain endothelial cells. Cel.l Mol. Neurobiol. 30, 727-735

Nakagawa, S., Deli, M.A., Nakao, S., Honda, M., Hayashi, K., Nakaoke, R., Kataoka, Y., Niwa, M., 2007. Pericyte from brain microvessels strengthen the barrier integrity in primary cultures of rat brain endothelial cells. Cel.l Mol. Neurobiol. 27, 687-694

Nakagawa, S., Deli, M.A., Kawaguchi, H., Shimizudani, T., Shimono, T., Kettel, A., Tanaka, K., Niwa, M., 2009. A new blood-brain barrier model using primary rat brain endothelial cells, pericytes and astrocytes. Neurochem. Int. 54, 253-263

Niiya, Y., Abumiya, T., Yamagishi, S., Takino, J., Takeuchi, M., 2012. Advanced glycation end products increase permeability of brain microvacular endothelial cells through reactive oxygen species-induced vascular endothelial growth factor expression. J. Stroke Cerebrovasc. Dis. 21, 293-298

Nitta, T., Hata, M., Gotoh, S., Seo, Y., Sasaki, H., Hashimoto, N., Furuse, M., Tsukita, S., 2003. Size-selective loosening of the blood-brain barrier in claudin-5-deficient mice. J. Cell Biol. 161, 653-660

Noda, K., Zhang, J., Fukuhara, S., Kunimoto, S., Yoshimura, M., Mochizuki, N., 2010. Vascular endothelial-cadherin stabilizes at cell-cell junctions by anchoring to circumferential actin bundles through α- and β-catenins in cyclic AMP-Epac-Rap1 signal-activated endothelial cells. Mol. Biol. Cell 21, 584-596

Perriere, N., Demeuse, P., Garcia, E., Regina, A., Debray, M., Andreux, J.P., Couvreur, P., Scherrmann, J.M., Temsamani, J., Couraud, P.O., Deli, M.A., Roux, F., 2005. Puromycin-based purification of rat brain capillary endothelial cell cultures. Effect on the expression of blood-brain barrier–specific properties. J. Neurochem. 93, 279-289

Ronaldson, P.T., Demarco, K.M., Sanchez-Covarrubias, L., Solinsky, CM., Davis, T.P.. 2009. Transforming growth factor-beta signaling alters substrate permeability and tight junction protein expression at the blood-brain barrier during inflammatory pain. J Cereb Blood Flow Metab. 29, 1084-1098

Schiller, M., Dennler, S., Anderegg, U., Kokot, A., Simon, J.C., Luger, T.A., Mauviel, A., Böhm, M., 2010. Increased cAMP levels modulate transforming growth factor-beta/Smad-induced expression of extracellular matrix components and other key fibroblast effector functions. J. Biol. Chem. 285, 409-421

Shen, W., Li, S., Chung, S.H., Zhu, L., Stayt, J., Su, T., Couraud, P.O., Romero, I.A., Weksler, B., Gillies, M.C., 2011. Tyrosine phosphorylation of VE-cadherin and claudin-5 is associated with TGF-β1-induced permeability of centrally derived vascular endothelium. Eur. J. Cell Biol. 90, 323-332

Shimizu, F., Sano, Y., Haruki, H., Kanda, T., 2011. Advanced glycation end-products induce basement membrane hypertrophy in endothelial microvessels and disrupt the blood-nerve barrier by stimulating the release of TGF-β and vascular endothelial growth factor (VEGF) by pericytes. Diabetologia 54, 1517-1526

Shimizu, F., Sano, Y., Tominaga, O., Maeda, T., Abe, M.A., Kanda, T., 2013. Advanced glycation end-products disrupt the blood-brain barrier by stimulating the release of transforming growth

factor-β by pericytes and vascular endothelial growth factor and matrix met alloproteinase-2 by endothelial cells in vitro. Neurobiol. Aging 34, 1902-1912

Shinohara, Y., Katayama, Y., Uchiyama, S., Yamaguchi, T., Handa, S., Matsuoka, K., Ohashi, Y., Tanahashi, N., Yamamoto, H., Genka, C., Kitagawa, Y., Kusuoka, H., Nishimaru, K., Tsushima, M., Koretsune, Y., Sawada, T., Hamada, C.; CSPS 2 group., 2010. Cilostazol for preventation of secondary stroke (CSPS 2): an aspirin-controlled, double-blind, randomized non-inferiority trial. Lancet Neurol. 9, 959-968

Starr J.M., Wardlaw J., Ferguson K., Maclulich A., Deary I.J., Marshall L., 2003. Increased blood-brain barrier permeability in type II diabetes demonstrated by gadolinium magnetic resonance imaging. J. Neurol. Neurosurg. Psychiatry. 74, 70-76

Togo, S., Liu, X., Wang, X., Sugiura, H., Kamio, K., Kawasaki, S., Kobayashi, T., Ertl, R.F., Ahn, Y., Holz, O., Magnussen, H., Fredriksson, K., Skold, C. M., Rennard, S.I., 2009. PDE4 inhibitors roflumilast and rolipram augment PGE2 inhibition of TGF-β1-stimulated fibroblasts. Am. J. Physiol. Lung Cell. Mol. Physiol. 296, L959-969

Torii, H., Kubota, H., Ishihara, H., Suzuki, M., 2007. Cilostazol inhibits the redistribution of the actin cytoskeleton and junctional proteins on the blood-brain barrier under hypoxia/reoxygenation. Pharmacol. Res. 55, 104-110

Tsukita, S., Furuse, M., Itoh, M., 2001. Multifunctional strands in tight junctions. Nat. Rev. Mol. Cell Biol. 2, 285 -293

Tsukita, S., Yamazaki, Y., Katsuno, T., Tamura, A., Tsukita, S., 2008. Tight junction-based epithelial microenvironment and cell proliferation. Oncogene. 27, 6930-6938

Tsuruya, R., Fujita, M., Ono, T., Koga, Y., Koga, Y., Yamamoto, T., Nanba, M., Shitara, M., Kasaoka, S., Maruyama, I., Yuasa, M., Maekawa, T., 2010. Hyperglycemia enhances excessive superoxide anion radical generation, oxidative stress, early inflammation, and endothelial injury in forebrain ischemia/reperfusion rats. Brain Res. 1309, 155-1563

Tureyen, K., Bowen, K., Liang, J., Dempsey, R.J., Vemuqati, R., 2011. Exacerbated brain damage, edema and inflammation in type-2 diabetic mice subjected to focal ischemia. J. Neurochem. 116, 499-507

Vannucci, S.J., Willing, L.B., Goto, S., Alkayed, N.J., Brucklacher, R.M., Wood, T.L., Towfighi, J., Hurn, P.D., Simpson, I.A., 2001. Experimental stroke in the female diabetic, db/db mouse. J. Cereb. Blood Flow Metab. 21, 52 -60

Vinik, A., Flemmer, M., 2002. Diabetes and macrovascular disease. J. Diabetes Complications 16, 235 – 245

Wang, X., Yan, L., Chen, W., Xu, L., Zhang, X., 2009. The renal protective effects of cilostazol on suppressing pathogenic thrombospondin-1 and transforming growth factor-beta expression in streptozotocin-induced diabetic rats. J. Int. Med. Res. 37, 145-153

Yamagishi, S., Fujimori, H., Yonekawa, H., Yamamoto, Y., Yamamoto, H., 1998. Advanced glycation end products inhibit prostacyclin production and induce plasminogen activator inhibitor-1 in human microvascular endothelial cells. Diabetologia 41, 1435-1441

Yan, F.L., Zheng, Y., Zhao, F.D., 2008. Effects of ginkgo biloba extract EGb761 on expression of RAGE and LRP-1 in cerebral microvascular endothelial cells under chronic hypoxia and hypoglycemia. Acta. Neuropathol. 116, 529-535

Yan, J., Zhang, Z., Shi, H., 2012. HIF - 1 is involved in high glucose - induced paracellular permeability of brain endothelial cells. Cell. Mol. Life Sci. 69, 115-128

Zhai, D.X., Kong, Q.F., Xu, W.S., Bai, S.S., Peng, H.S., Zhao, K., Li, G.Z., Wang, D.D., Sun, B., Wang, J.H., Wang, G.Y., Li, H.L., 2008. RAGE expression is up-regulated in human cerebral ischemia and pMCAO rats. Neurosci. Lett. 445, 117-121

Figure legends

Fig. 1 Schematic drawing of the preparation of the *in vitro* BBB model, and experimental procedure. Rat brain capillary endothelial cells (RBEC) were isolated 4 days before the establishment of the *in vitro* BBB model. To purify cultures, cells were kept in the presence of puromycin (4 μg/mL) for 2 days (RBEC I medium + puromycin). Rat astrocytes were seeded at the bottom of 12-well plates, while rat pericytes at the filter membranes of inverted cell culture inserts the day before the start of the co-culture. On Day 4, RBEC were plated on the top of polycarbonate membranes of 12-well Transwell® inserts. From Day 5, RBEC were grown in culture medium containing 500 nM hydrocortisone (RBEC II medium + hydrocortisone). Experiments were performed on Day 8. In order to initiate normoxia or oxygen glucose deprivation (OGD), DMEM containing 17.5 mM glucose (glucose+ DMEM) or glucose-free DMEM (glucose- DMEM) was used in the *in vitro* BBB model, respectively. Three-hour hypoxia was generated using AnaeroPack®. Reoxygenation was initiated by adding RBEC II medium with or without 10 μM cilostazol and 200 μg/mL AGEs for 24 h.

Fig. 2 Effects of advanced glycation endproducts (AGEs) on transendothelial electrical resistance (TEER) in *in vitro* blood-brain barrier (BBB) model. (a) BBB model was exposed to bovine serum albumin (BSA, 200 μg/mL) or AGEs (200 μg/mL) under normoxia for 24 h (open and light gray columns, respectively*)*. Values are shown as rate of change in TEER before and after treatment in comparison with BSA. TEER in normoxia BSA before treatment was 283 ± 14.5 Ω × cm^2. No significant differences in TEER were observed between BSA and AGEs under normoxia. BBB model was exposed to BSA or AGEs under 3 h oxygen glucose deprivation (OGD)/24 h reoxygenation (dark gray column and black column, respectively). TEER was significantly lower under 3-h OGD/24-h reoxygenation than under normoxia

($^{**}p < 0.01$ vs. normoxia BSA-control). Treatment of AGEs significantly decreased TEER under 3-h OGD/24-h reoxygenation ($^{\#\#}p < 0.01$). All data are presented as means ± SEM ($n = 5 \sim 11$). (b) Western blot analysis of receptor for AGEs (RAGE) expression in rat brain capillary endothelial cells (RBEC) of *in vitro* BBB model treated with BSA under normoxia and 3-h OGD/24-h reoxygenation. Bar graph reflects combined densitometry data (mean ± SEM, $n = 6$). Expression of RAGE was significantly elevated after 3-h OGD/24-h reoxygenation (black column, $^{*}p < 0.05$ vs. normoxia).

Fig. 3 Effects of cilostazol on transendothelial electrical resistance (TEER) *in vitro* blood-brain barrier (BBB) model treated with advanced glycation endproducts (AGEs) under normoxia and 3 h oxygen glucose deprivation (OGD)/24 h reoxygenation. Cilostazol (10 μM) had no effect on TEER under normoxia when compared with 200 μg/mL bovine serum albumin (BSA)-control at 24 hours. BBB models were subjected to 3 h oxygen glucose deprivation (3 h OGD)/ 24 h reoxygenation. After 3-h OGD/24-h reoxygenation, treatment of AGEs (200 μg/mL) significantly decreased TEER ($^{*}p < 0.05$ vs. BSA). A significant increase in TEER was observed in rat brain capillary endothelial cells (RBEC) treated with 10 μM cilostazol for 3-h OGD/24-h reoxygenation ($^{\#}p < 0.05$ vs. 3-h OGD/24-h reoxygenation AGEs). TEER values are expressed as percentage of normoxia BSA-control value (100% = 250 ± 16.6). All data are presented as means ± SEM ($n = 7 \sim 8$).

Fig. 4 Expression of tight junction protein in RBEC in *in vitro* blood-brain barrier (BBB) model. Immunofluorescent staining showed that the expression of claudin-5 was disrupted in rat brain capillary endothelial cells (RBEC) of BBB model with 3 h oxygen glucose deprivation (OGD)/24 h reoxygenation (b) compared with normoxic controls (a). Arrows indicate the changes in claudin-5 distribution. Moreover, advanced glycation endproducts (AGEs, 200 μg/mL) enhanced disruption of the expression of claudin-5 under 3-h OGD/24-h reoxygenation (c). Asterisks (*) indicate the disruption of claudin-5. Cilostazol

restored the expression of claudin-5 (d). Bar = 10 μm. Expression of zonula occludens protein-1 (ZO-1) in RBEC of the *in vitro* BBB model were examined by immunofluorescent staining. There were no significant differences between the images of ZO-1 (e: normoxia, f: OGD/reoxygenation, g: OGD/reoxygenation with AGEs, h: OGD/reoxygenation with AGEs and cilostazol). Bar = 10 μm. (i) Western blot analysis of claudin-5 in RBEC of the BBB model with normoxia or 3-h OGD/24-h reoxygenation. Treatment of AGEs significantly decreased the expression of claudin-5 after 3-h OGD/24-h reoxygenation (dark gray column, $^{*}p < 0.05$ vs. normoxia bovine serum albumin (BSA)). However, significant decreases in the expression of claudin-5 were not observed in BSA and AGEs treated with 10 μM cilostazol after 3-h OGD/24-h reoxygenation (light gray and black column, vs. normoxia BSA). Blots are representative images from three separate experiments, and graphs represent densitometric measurements from these experiments. Values are means ± SEM ($n = 11 \sim 15$). (j) Western blot analysis of ZO-1 in RBEC of the BBB model with normoxia or 3-h OGD/24-h reoxygenation. The bar graph reflects the combined densitometry data (mean ± SEM, $n = 5$). There were no significant differences in expression of ZO-1 between BSA, AGEs and AGEs treated with 10 μM cilostazol after 3-h OGD/24-h reoxygenation.

Fig. 5 Involvement of transforming growth factor (TGF)-β1 in advanced glycation endproduct (AGE)-induced blood-brain barrier (BBB) dysfunction under oxygen glucose deprivation (OGD) and reoxygenation. (a) Rat brain capillary endothelial cells (RBEC) were incubated with the bovine serum albumin (BSA, 200 μg/mL) or AGEs (200 μg/mL) under 3-h OGD/24-h reoxygenation in the absence or presence of cilostazol (10 μM). TGF-β1 level in medium was determined using a TGF-β1 ELISA kit. A significant increase in TGF-β1 was observed on the luminal side of the BBB model with 3-h OGD/24-h reoxygenation (light gray column, $*p < 0.05$ vs. normoxia BSA). Moreover, AGEs enhanced the secretion of TGF-β1 on the luminal side of the BBB model induced by 3-h OGD/24-h reoxygenation (dark gray

column, **$p < 0.01$ vs. normoxia BSA, $^{\#\#}p < 0.01$ vs. OGD/reoxygenation BSA). Cilostazol inhibited AGE-induced increases in TGF-β1 under 3-h OGD/24-h reoxygenation (black column, ##$p < 0.01$ vs. OGD/reoxygenation AGEs). Data are shown as means ± SEM. ($n = 3$). (b) *In vitro* BBB models were exposed to A83-01, a selective inhibitor of TGF-β receptor, together with BSA or AGEs under 3-h OGD/24-h reoxygenation. Decreases in TEER induced by AGEs were improved in the presence of A83-01 (**$p < 0.01$ vs. BSA, $^{\#\#}p < 0.01$ vs. AGEs). TEER values were expressed as a percentage of control values (mean ± SEM, $^{**}p < 0.01$ in comparison between BSA and AGEs, $n = 6 \sim 10$).

Fig. 6 Effects of transforming growth factor (TGF)-β1 on the transendothelial electrical resistance (TEER) *in vitro* blood-brain barrier (BBB) model. BBB models were exposed to TGF-β1 (1 ng/mL) under normoxia. Treatment of TGF-β1 significantly decreased TEER when compared with controls ($^{**}p < 0.01$ vs. control). The decrease in TEER induced by TGF-β1 was improved in the presence of 10 μM cilostazol ($^{\#}p < 0.05$, $^{\#\#}p < 0.01$ TGF-β1 vs. TGF-β1 + cilostazol). TEER was measured at 3, 6, 9, 12 or 24 h, and values are expressed as a percentage of control values (mean ± SEM, $n = 6$).

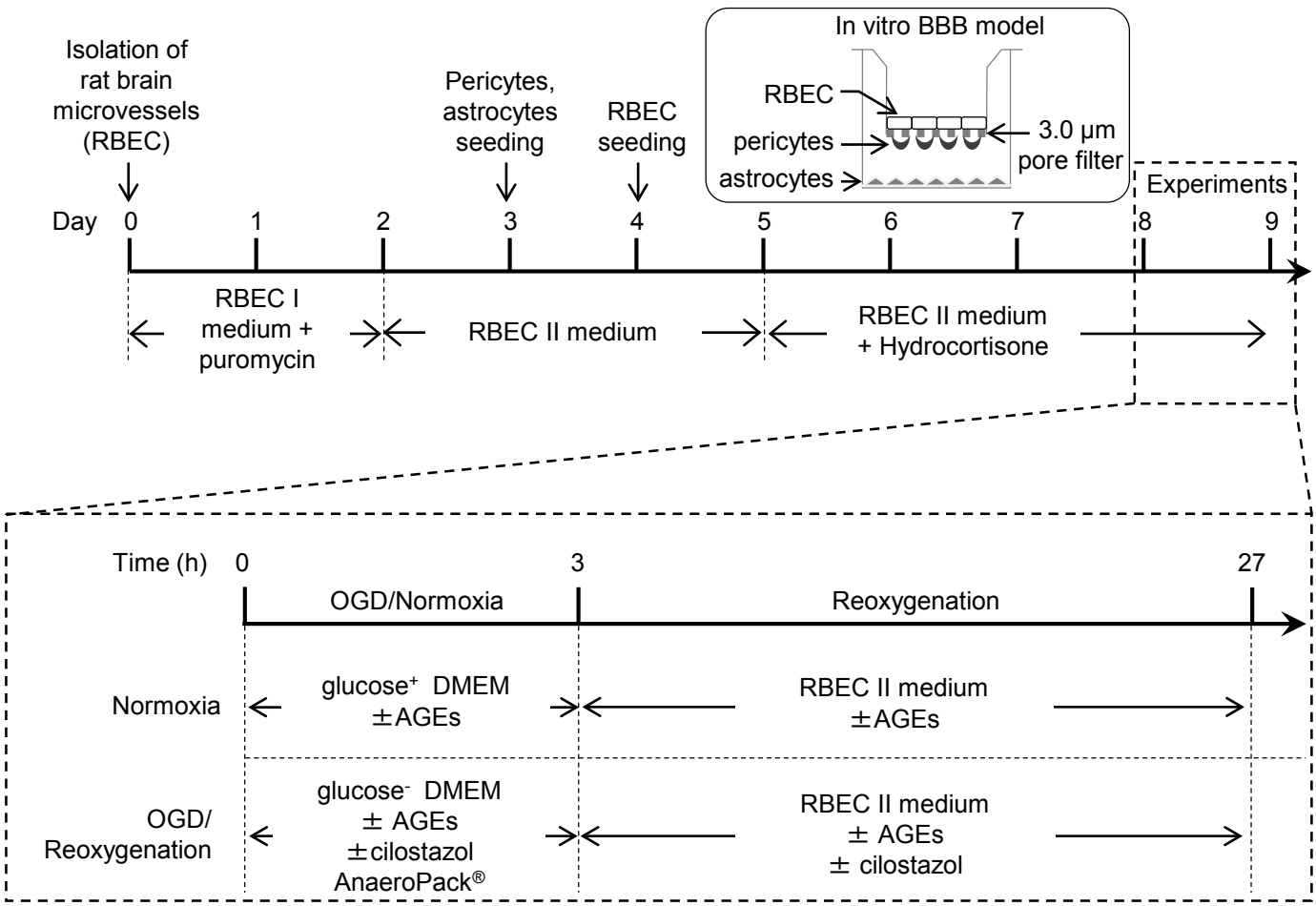
Isolation of rat brain microvessels (RBEC)
Pericytes, astrocytes seeding
RBEC seeding
In vitro BBB model
RBEC
pericytes
astrocytes
3.0 µm pore filter
Experiments
Day 0 1 2 3 4 5 6 7 8 9
RBEC I medium + puromycin
RBEC II medium
RBEC II medium + Hydrocortisone
Time (h) 0 3 27
OGD/Normoxia
Reoxygenation
Normoxia
glucose+ DMEM ±AGEs
RBEC II medium ±AGEs
OGD/ Reoxygenation
glucose- DMEM ± AGEs ±cilostazol AnaeroPack®
RBEC II medium ± AGEs ± cilostazol

Fig. 1

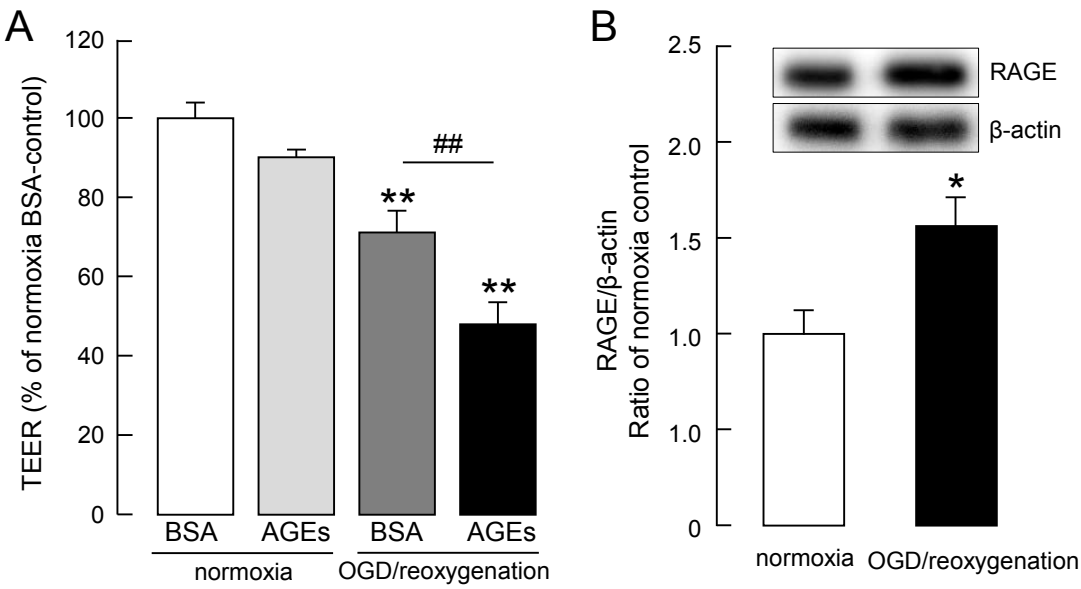
A
TEER (% of normoxia BSA-control)
120
100
80
60
40
20
0
##
**
**
BSA
AGEs
BSA
AGEs
normoxia
OGD/reoxygenation
B
RAGE/β-actin
Ratio of normoxia control
2.5
2.0
1.5
1.0
1.0
0
RAGE
β-actin
*
normoxia
OGD/reoxygenation

Fig. 2

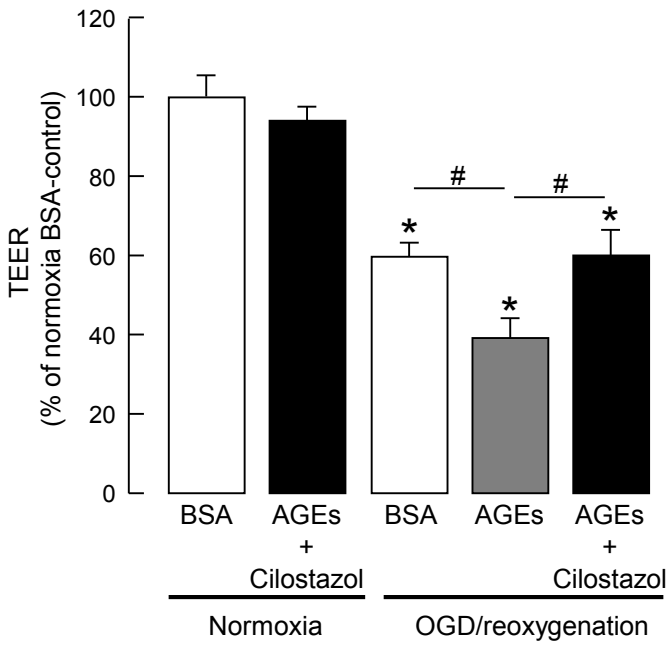
120
100
80
60
40
20
0
TEER
(% of normoxia BSA-control)
#
#
*
*
*
BSA
AGEs
+
Cilostazol
BSA
AGEs
AGEs
+
Cilostazol
Normoxia
OGD/reoxygenation

Fig. 3

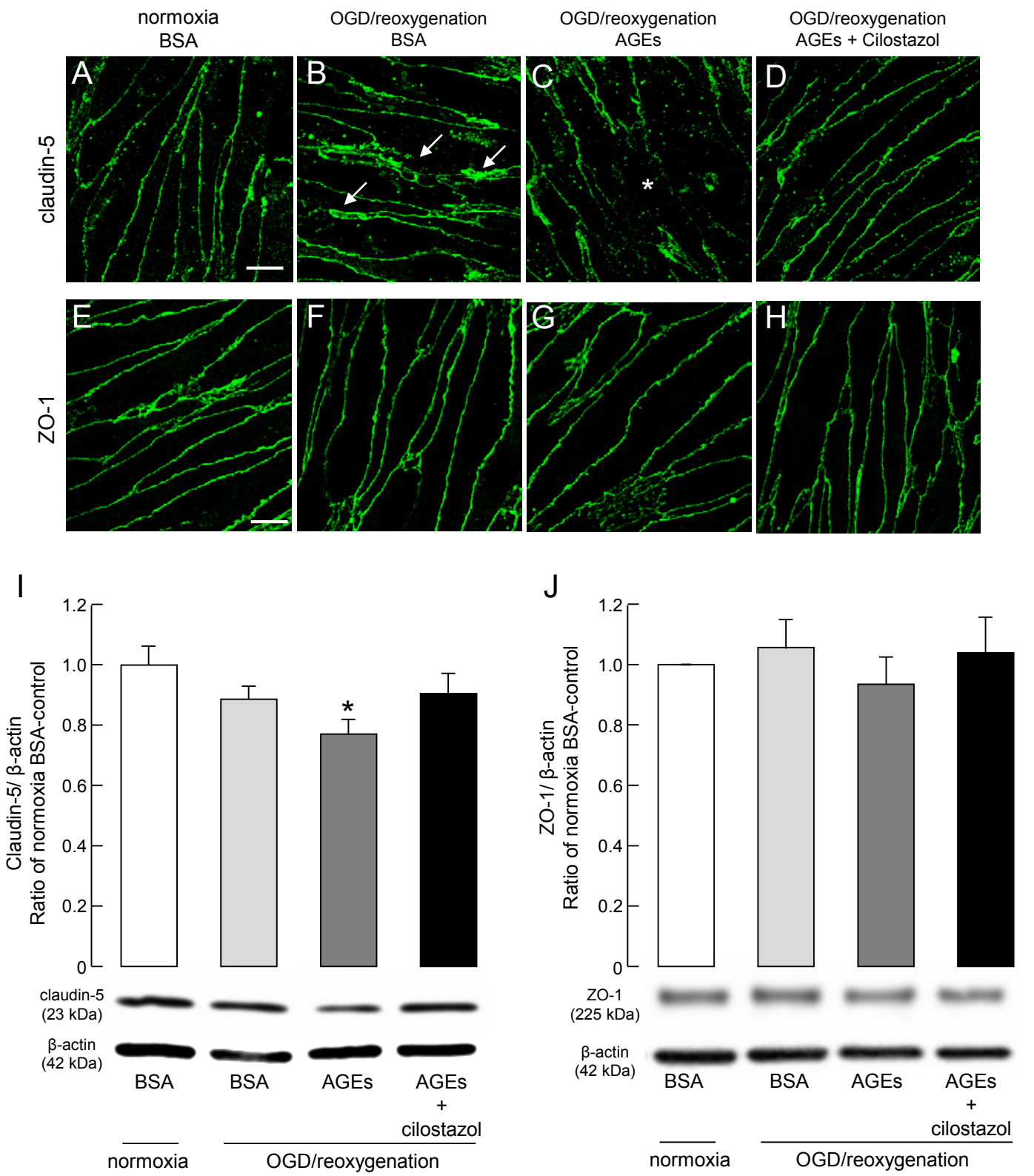
normoxia
BSA
OGD/reoxygenation
BSA
OGD/reoxygenation
AGEs
OGD/reoxygenation
AGEs + Cilostazol
A
B
C
D
claudin-5
E
F
G
H
ZO-1
I
Claudin-5/ β-actin
Ratio of normoxia BSA-control
1.2
1.0
0.8
0.6
0.4
0.2
0
*
claudin-5
(23 kDa)
β-actin
(42 kDa)
BSA
BSA
AGEs
AGEs
+
cilostazol
normoxia
OGD/reoxygenation
J
ZO-1/ β-actin
Ratio of normoxia BSA-control
1.2
1.0
0.8
0.6
0.4
0.2
0
ZO-1
(225 kDa)
β-actin
(42 kDa)
BSA
BSA
AGEs
AGEs
+
cilostazol
normoxia
OGD/reoxygenation

Fig. 4

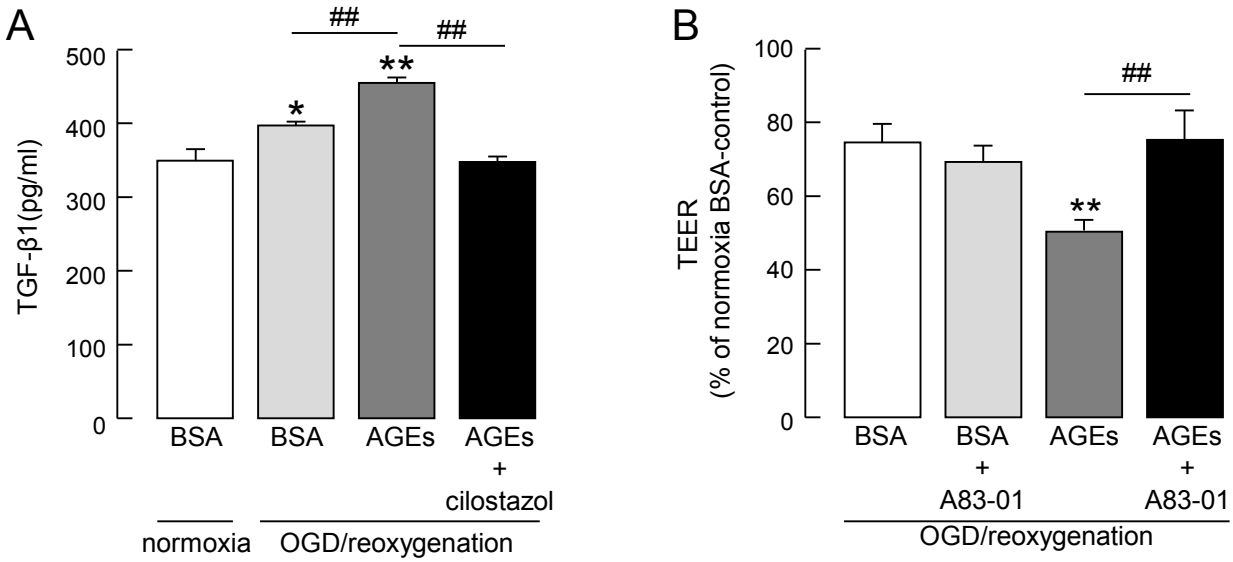
A
TGF-β1(pg/ml)
500
400
300
200
100
0
##
##
*
**
BSA
BSA
AGEs
AGEs
+
cilostazol
normoxia
OGD/reoxygenation
B
TEER
(% of normoxia BSA-control)
100
80
60
40
20
0
##
**
BSA
BSA
+
A83-01
AGEs
AGEs
+
A83-01
OGD/reoxygenation

Fig. 5

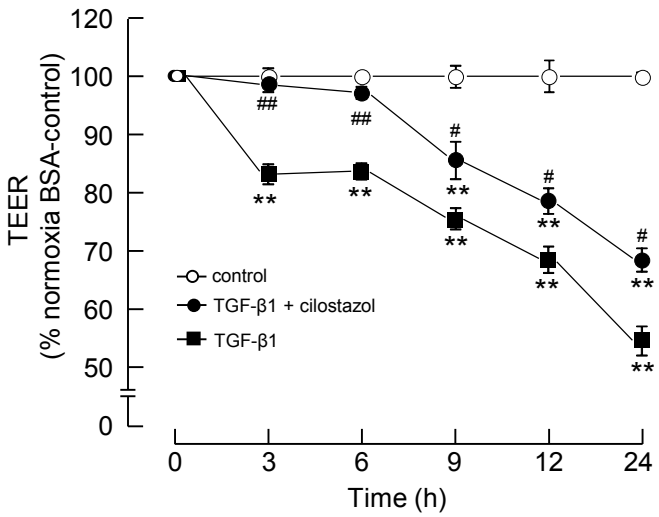
120
100
90
80
70
60
50
0
TEER
(% normoxia BSA-control)
control
TGF-β1 + cilostazol
TGF-β1
0
3
6
9
12
24
Time (h)
##
##
#
#
#
**
**
**
**
**
**

Fig. 6